

DRAFT VERSION FEBRUARY 5, 2007

Preprint typeset using L<sup>A</sup>T<sub>E</sub>X style emulateapj v. 12/01/06CONSTRAINTS ON THE STEADY AND PULSED VHE  $\gamma$ -RAY EMISSION FROM OBSERVATION OF PSR B1951+32 / CTB 80 WITH THE MAGIC TELESCOPE

J. ALBERT<sup>A</sup>, E. ALIU<sup>B</sup>, H. ANDERHUB<sup>C</sup>, P. ANTORANZ<sup>D</sup>, A. ARMADA<sup>B</sup>, C. BAIXERAS<sup>E</sup>, J. A. BARRIO<sup>D</sup>, H. BARTKO<sup>F</sup>, D. BASTIERI<sup>G</sup>, J. K. BECKER<sup>H</sup>, W. BEDNAREK<sup>I</sup>, K. BERGER<sup>A</sup>, C. BIGONGIARI<sup>G</sup>, A. BILAND<sup>C</sup>, R. K. BOCK<sup>F,G</sup>, P. BORDAS<sup>J</sup>, V. BOSCH-RAMON<sup>J</sup>, T. BRETZ<sup>A</sup>, I. BRITVITCH<sup>C</sup>, M. CAMARA<sup>D</sup>, E. CARMONA<sup>F</sup>, A. CHILINGARIAN<sup>K</sup>, S. CIPRINI<sup>L</sup>, J. A. COARASA<sup>F</sup>, S. COMMICHIAU<sup>C</sup>, J. L. CONTRERAS<sup>D</sup>, J. CORTINA<sup>B</sup>, M.T. COSTADO<sup>M</sup>, V. CURTEF<sup>H</sup>, V. DANIELYAN<sup>K</sup>, F. DAZZI<sup>G</sup>, A. DE ANGELIS<sup>N</sup>, C. DELGADO<sup>M</sup>, R. DE LOS REYES<sup>D</sup>, B. DE LOTTO<sup>N</sup>, E. DOMINGO-SANTAMARÍA<sup>B</sup>, D. DORNER<sup>A</sup>, M. DORO<sup>G</sup>, M. ERRANDO<sup>B</sup>, M. FAGIOLINI<sup>O</sup>, D. FERENC<sup>P</sup>, E. FERNÁNDEZ<sup>B</sup>, R. FIRPO<sup>B</sup>, J. FLIX<sup>B</sup>, M. V. FONSECA<sup>D</sup>, L. FONT<sup>E</sup>, M. FUCHS<sup>F</sup>, N. GALANTE<sup>F</sup>, R. GARCÍA-LÓPEZ<sup>M</sup>, M. GARCZARCZYK<sup>F</sup>, M. GAUG<sup>G</sup>, M. GILLER<sup>I</sup>, F. GOEBEL<sup>F</sup>, D. HAKOBYAN<sup>K</sup>, M. HAYASHIDA<sup>F</sup>, T. HENGSTEBECK<sup>Q</sup>, A. HERRERO<sup>M</sup>, K. HIROTANI<sup>V</sup>, D. HÖHNE<sup>A</sup>, J. HOSE<sup>F</sup>, C. C. HSU<sup>F</sup>, P. JACON<sup>I</sup>, T. JOGLER<sup>F</sup>, O. KALEKIN<sup>Q</sup>, R. KOSYRA<sup>F</sup>, D. KRANICH<sup>C</sup>, R. KRITZER<sup>A</sup>, A. LAILLE<sup>P</sup>, P. LIEBING<sup>F</sup>, E. LINDFORS<sup>L</sup>, S. LOMBARDI<sup>G</sup>, F. LONGO<sup>N</sup>, J. LÓPEZ<sup>B</sup>, M. LÓPEZ<sup>D</sup>, E. LORENZ<sup>C,F</sup>, P. MAJUMDAR<sup>F</sup>, G. MANEVA<sup>R</sup>, K. MANNHEIM<sup>A</sup>, O. MANSUTTI<sup>N</sup>, M. MARIOTTI<sup>G</sup>, M. MARTÍNEZ<sup>B</sup>, D. MAZIN<sup>F</sup>, C. MERCK<sup>F</sup>, M. MEUCCI<sup>O</sup>, M. MEYER<sup>A</sup>, J. M. MIRANDA<sup>D</sup>, R. MIRZOYAN<sup>F</sup>, S. MIZOBUCHI<sup>F</sup>, A. MORALEJO<sup>B</sup>, K. NILSSON<sup>L</sup>, J. NINKOVIC<sup>F</sup>, E. OÑA-WILHELM<sup>B</sup>, N. OTTE<sup>F,\*</sup>, I. OYA<sup>D</sup>, D. PANEQUE<sup>F</sup>, M. PANNIELLO<sup>M</sup>, R. PAOLETTI<sup>O</sup>, J. M. PAREDES<sup>J</sup>, M. PASANEN<sup>L</sup>, D. PASCOLI<sup>G</sup>, F. PAUSS<sup>C</sup>, R. PEGNA<sup>O</sup>, M. PERSIC<sup>N,S</sup>, L. PERUZZO<sup>G</sup>, A. PICCIOLI<sup>O</sup>, M. POLLER<sup>A</sup>, N. PUCHADES<sup>B</sup>, E. PRANDINI<sup>G</sup>, A. RAYMERS<sup>K</sup>, W. RHODE<sup>H</sup>, M. RIBÓ<sup>J</sup>, J. RICO<sup>B</sup>, M. RISSI<sup>C</sup>, A. ROBERT<sup>E</sup>, S. RÜGAMER<sup>A</sup>, A. SAGGION<sup>G</sup>, A. SÁNCHEZ<sup>E</sup>, P. SARTORI<sup>G</sup>, V. SCALZOTTO<sup>G</sup>, V. SCAPIN<sup>G</sup>, R. SCHMITT<sup>A</sup>, T. SCHWEIZER<sup>F</sup>, M. SHAYDUK<sup>Q,F</sup>, K. SHINOZAKI<sup>F</sup>, S. N. SHORE<sup>T</sup>, N. SIDRO<sup>B</sup>, A. SILLANPÄÄ<sup>N</sup>, D. SOBCHYNSKA<sup>I</sup>, A. STAMERRA<sup>O</sup>, L. S. STARK<sup>C</sup>, L. TAKALO<sup>L</sup>, P. TEMNIKOV<sup>R</sup>, D. TESCARO<sup>B</sup>, M. TESHIMA<sup>F</sup>, N. TONELLO<sup>F</sup>, D. F. TORRES<sup>B,U</sup>, N. TURINI<sup>O</sup>, H. VANKOV<sup>R</sup>, V. VITALE<sup>N</sup>, R. M. WAGNER<sup>F</sup>, T. WIBIG<sup>I</sup>, W. WITTEK<sup>F</sup>, R. ZANIN<sup>B</sup>, J. ZAPATERO<sup>E</sup>

Draft version February 5, 2007

## ABSTRACT

We report on VHE  $\gamma$ -observations with the MAGIC telescope of the pulsar PSR B1951+32 and its associated nebula CTB 80. Our data constrain the cutoff energy of the pulsar to be  $< 32$  GeV, assuming the pulsed  $\gamma$ -ray emission to be exponentially cutoff. The upper limit on the flux of pulsed  $\gamma$ -ray emission  $> 75$  GeV is  $4.3 \cdot 10^{-11}$  photons  $\text{cm}^{-2} \text{sec}^{-1}$  and the upper limit on the flux of steady emission  $> 140$  GeV is  $1.5 \cdot 10^{-11}$  photons  $\text{cm}^{-2} \text{sec}^{-1}$ . We discuss our results in the framework of recent model predictions and other studies.

*Subject headings:* CTB 80, PSR B1951+32, Pulsar wind nebula, Pulsar

## 1. INTRODUCTION

It is currently believed that pulsars are among the few objects in our Galaxy that are candidate sources of ultra relativistic charged cosmic rays. Relativistic particles within the magnetosphere emit  $\gamma$ -rays up to energies of several GeV in various processes like Curvature, Synchrotron radiation and Inverse Compton (IC) scattering. Thus, observations in the multi-GeV  $\gamma$ -ray domain allow to study the acceleration sites in the magnetosphere of the pulsar. Predicted sites where particle acceleration can take place are e.g. above the polar cap of the neutron star (e.g. Harding et al. 1978; Daugherty and Harding 1982) or in the so-called outer gap of the magnetosphere (e.g. Cheng et al. 1986b,a; Chiang and Romani 1992). Furthermore, particle acceleration can take place outside the magnetosphere in the region where the pulsar wind interacts with the interstellar medium. If electrons are accelerated in these shocks they could give rise to IC-scattered photons from e.g. the cosmic microwave background, synchrotron radiation or thermal origin (de Jager and Harding 1992; Atayan and Aharonian 1996; Bednarek and Bartosik 2003).

PSR B1951+32 was detected first at radio frequencies by Kulkarni et al. (1988), and is one of the six rotation-powered high energy pulsars whose GeV emission was detected by EGRET (Ramanamurthy et al. 1995). Among  $\gamma$ -ray pulsars, PSR B1951+32 is the only source observed to emit up to 20 GeV with no cutoff being evident in the differential energy spectrum. The spectrum shows a hard

<sup>a</sup> Universität Würzburg, D-97074 Würzburg, Germany<sup>b</sup> Institut de Física d'Altes Energies, Edifici Cn., E-08193 Bellaterra (Barcelona), Spain<sup>c</sup> ETH Zurich, CH-8093 Switzerland<sup>d</sup> Universidad Complutense, E-28040 Madrid, Spain<sup>e</sup> Universitat Autònoma de Barcelona, E-08193 Bellaterra, Spain<sup>f</sup> Max-Planck-Institut für Physik, D-80805 München, Germany<sup>g</sup> Università di Padova and INFN, I-35131 Padova, Italy<sup>h</sup> Universität Dortmund, D-44227 Dortmund, Germany<sup>i</sup> University of Łódź, PL-90236 Łódź, Poland<sup>j</sup> Universitat de Barcelona, E-08028 Barcelona, Spain<sup>k</sup> Yerevan Physics Institute, AM-375036 Yerevan, Armenia<sup>l</sup> Tuorla Observatory, Turku University, FI-21500 Piikkiö, Finland<sup>m</sup> Instituto de Astrofísica de Canarias, E-38200, La Laguna, Tenerife, Spain<sup>n</sup> Università di Udine, and INFN Trieste, I-33100 Udine, Italy<sup>o</sup> Università di Siena, and INFN Pisa, I-53100 Siena, Italy<sup>p</sup> University of California, Davis, CA-95616-8677, USA<sup>q</sup> Humboldt-Universität zu Berlin, D-12489 Berlin, Germany<sup>r</sup> Institute for Nuclear Research and Nuclear Energy, BG-1784 Sofia, Bulgaria<sup>s</sup> INFN/Osservatorio Astronomico and INFN Trieste, I-34131 Trieste, Italy<sup>t</sup> Università di Pisa, and INFN Pisa, I-56126 Pisa, Italy<sup>u</sup> ICREA and Institut de Ciències de l'Espai, IEEC-CSIC, E-08193 Bellaterra, Spain<sup>v</sup> ASIAA/National Tsing Hua University - TIARA, PO Box 23-141, Taipei, Taiwan, R. O. C.<sup>\*</sup> Corresponding author, [otte@mppmu.mpg.de](mailto:otte@mppmu.mpg.de)

TABLE 1

SUMMARY OF THE OBSERVATION OF PSR B1951+32 WITH MAGIC. THE EXTINCTION COEFFICIENTS ARE TAKEN FROM PUBLICLY AVAILABLE DATA OF THE CARLSBERG MERIDIAN TELESCOPE THAT IS LOCATED ON THE SAME SITE AS MAGIC. THE EXTINCTION COEFFICIENT IS FOR AN EFFECTIVE WAVELENGTH OF 625NM.

Date	Rates [Hz]	On Time [min]	Ext. Coef. [mag]	Sc. Ext. Coef. [mag]	selected
04.07.2006	164	130	0.099	0.017	yes
05.07.2006	164	136	0.100	0.011	yes
06.07.2006	167	105	0.088	0.014	yes
07.07.2006	176	62	0.091	0.011	yes
03.08.2006	151	95	0.161	0.009	yes
04.08.2006	n.a.	n.a.	0.266	0.045	no
23.08.2006	175	168	0.079	0.017	yes
24.08.2006	158	105	0.088	0.014	yes
25.08.2006	165	138	0.142	0.029	yes
26.08.2006	135	148	0.168	0.044	no
27.08.2006	167	124	0.140	0.042	yes
28.08.2006	n.a.	n.a.	0.249	0.056	no
13.09.2006	147	83	n.a	n.a	yes
14.09.2006	139	155	0.105	0.016	yes
15.09.2006	156	102	0.091	0.017	yes
16.09.2006	147	125	0.095	0.013	yes
17.09.2006	149	89	0.094	0.060	yes

spectral index of 1.8 between 100 MeV and 20 GeV. The pulsar has an apparent high efficiency ( $\sim 0.4\%$ ) of converting its rotational energy loss rate,  $3.7 \times 10^{36} \text{ ergs s}^{-1}$ , into  $\gamma$ -rays  $> 100 \text{ MeV}$  (assuming a distance of 2.5 kpc to the pulsar). Moreover, the  $\gamma$ -ray luminosity at  $\sim 10 \text{ GeV}$  is comparable to the Crab pulsar (Ramanamurthy et al. 1995).

Inferred from its rotational parameters the spin down age of PSR B1951+32 is  $\sim 10^5$  years (Manchester et al. 2005), i.e. about 100 times older than the Crab pulsar. The magnetic field strength of  $4.9 \cdot 10^{11} \text{ G}$  (Manchester et al. 2005) is lower than in most rotation-powered pulsars. Based on some models (e.g. Harding et al. 1997) it is therefore expected that the screening of  $\gamma$ -rays due to pair production in the magnetosphere of PSR B1951+32 is reduced and the cut-off of the high energy emission subsequently shifts to higher energies. Based on these arguments, the pulsar PSR B1951+32 is a prime candidate for observation by ground based  $\gamma$ -ray detectors with low energy thresholds like the imaging air Cherenkov telescope MAGIC.

The pulsar is located in the core of the radio nebula CTB 80, which is thought to be physically associated with the pulsar. In X-rays the nebula shows a cometary shape (Moon et al. 2004; Li et al. 2005), being confined by a bow shock that is produced by the pulsar's high proper motion ( $240 \pm 40 \text{ km/s}$ ) (Migliazzo et al. 2002). Bednarek and Bartosik (2005b) predict a  $> 200 \text{ GeV}$  flux from the nebula at a level of  $\sim 4.4\%$  of the Crab flux, by assuming that high energy leptons can accumulate inside the well localized nebula for long periods of time as observed in the case of the Crab nebula.

The current tightest constraint on the  $> 100 \text{ GeV}$  emission from the pulsar and its nebula, obtained by the Whipple collaboration (Srinivasan et al. 1997), puts an upper limit, 75 GeV, on the cutoff energy of the pulsed emission and an upper limit,  $\leq 1.95 \times 10^{-11} \text{ cm}^{-2} \text{ s}^{-1}$ , on the  $> 260 \text{ GeV}$  steady emission. The latter is a factor  $\sim 2$  within the prediction of Bednarek and Bartosik (2005b).

In this paper we present upper limits on the cutoff en-

ergy of the pulsed emission from the pulsar, as well as on the steady and pulsed VHE fluxes from the region associated with the radio nebula, resulting from MAGIC telescope observations that were performed in July throughout September 2006. The paper is structured as follows: After a short introduction to MAGIC and our data taking and analysis (Section 2), we report about our search for steady and pulsed emission from PSR B1951+32 (Section 3). We close with a discussion of the implications of our results (Section 4).

## 2. OBSERVATIONS AND ANALYSIS

The MAGIC (Major Atmospheric Gamma Imaging Cherenkov) telescope, see Lorenz (2004), is located on the Canary Island La Palma (2200 m asl,  $28.45^\circ \text{N}$ ,  $17.54^\circ \text{W}$ ). MAGIC is currently the largest imaging atmospheric Cherenkov telescope (IACT), having a 17 m diameter tessellated reflector dish comprising 964  $0.5 \times 0.5 \text{ m}^2$  diamond-milled aluminium mirrors. The faint Cherenkov light flashes produced by air showers are recorded by the telescope camera, which consists of 577 photomultiplier tubes. Together with the current configuration of the MAGIC camera with a trigger region of 2.0 degrees diameter (Cortina et al. 2005), this results in a trigger collection area for  $\gamma$ -rays of about  $10^5 \text{ m}^2$  at small zenith angles. The effective collection area depends on the analysis and is  $\sim 10^4 \text{ m}^2$  around 60 GeV and increases to  $\gtrsim 6 \cdot 10^4 \text{ m}^2$  beyond 200 GeV. Presently, the minimum trigger energy is 50-60 GeV (at small zenith angles). The MAGIC telescope is focused to 10 km distance — the most likely position for a 50 GeV air shower maximum. The accuracy in reconstructing the direction of incoming  $\gamma$ -rays on an event by event basis (point spread function (PSF)), is about 0.1 degrees, slightly depending on energy and the chosen analysis method. A source with a  $\gamma$ -ray flux of  $\sim 2\%$  of the Crab nebula and the same spectral slope can be detected by MAGIC  $> 200 \text{ GeV}$  with a significance level of  $5 \sigma$  within 50 hours.

PSR B1951+32 was observed with MAGIC for a total of 17 nights between July 4<sup>th</sup> and September 17<sup>th</sup>, 2006. The observations were performed in the so-called ON/OFF mode, i.e. PSR B1951+32 was observed by di-

rectly pointing to it (ON). Three nights were rejected because of unstable trigger rates due to bad weather. The background was estimated by observing at the same zenith angle range for 5.8 hours a suitable region in the sky where no  $\gamma$ -ray source is expected (OFF). In total 30.7 hours of data were processed. The zenith angle range of the observation was restricted to between  $5^\circ$  and  $25^\circ$ , guaranteeing the lowest possible energy threshold. A summary of the observation gives Table 1. This table also includes atmospheric extinction coefficients of all nights, provided by the Carlsberg Meridian telescope, which is located at the same site as MAGIC.

Following calibration of the data (Gaug et al. 2005) and a tail-cut image cleaning of the events, a Hillas parametrization algorithm was applied (Hillas 1985). The tail-cuts used in the image cleaning were 6 photoelectrons for core-pixels and 4 photoelectrons for boundary-pixels. For the generation of sky maps we used tail-cuts of 10 and 5 photoelectrons. Additional suppression of pixels containing noise was achieved by requesting a narrow time coincidence between adjacent pixels ( $\sim 7$  nsec). The hadronic background was suppressed with a multivariate method, the Random Forest (Breiman 2001; Bock et al. 2004), that uses the Hillas parameters of an event to decide on its so-called HADRONNESS. The power to suppress hadronic background is energy dependent and reduced for  $\gamma$ -ray energies  $< 150$  GeV. As a consequence the optimal cut in HADRONNESS, which gives the highest rejection of background while retaining most of  $\gamma$ -ray candidates, has to be independently determined for each energy region. For the analysis of the data presented here we used an energy dependent HADRONNESS-cut, whose empirical parametrization was derived from Monte Carlo studies. An exception are the sky maps for which a static HADRONNESS-cut was applied in the event selection. This is justified as the maps were produced for energies  $> 200$  GeV where the dependence of the optimal HADRONNESS-cut on energy is small. The method of Random Forests is also used to estimate the energy of an event. Typically, energy resolutions of  $\sim 25\%$  are achieved on an event by event basis.

### 3. RESULTS

#### 3.1. Search for steady Emission

We searched for steady  $\gamma$ -ray emission of a point source from the direction of PSR B1951+32 with different analysis thresholds between 140 GeV and 2.6 TeV. We define the analysis threshold as the peak of the energy distribution of MC-events after cuts. Images of  $\gamma$ -rays from PSR B1951+32 point with their major axis to the camera center, and thus appear as an excess at small values in the parameter ALPHA. ALPHA is the angle between the major axis of the shower image and the direction determined by the image center of gravity and the camera center. In Figure 1 we show the  $|\text{ALPHA}|$ -distribution for events with energies  $\gtrsim 280$  GeV. An excess due to  $\gamma$ -ray emission from PSR B1951+32 should be visible in the figure for  $|\text{ALPHA}| < 7.5^\circ$ . The results of this analyses and other ones with different analysis thresholds summarizes Table 2. As no significant signal ( $> 5\sigma$ ) of  $\gamma$ -rays was found, we calculated upper limits on the number of excess events with a confidence level of 95% by using the method of Rolke et al. (2005). In the calculation of the limits a systematic uncertainty on the flux of 30% was

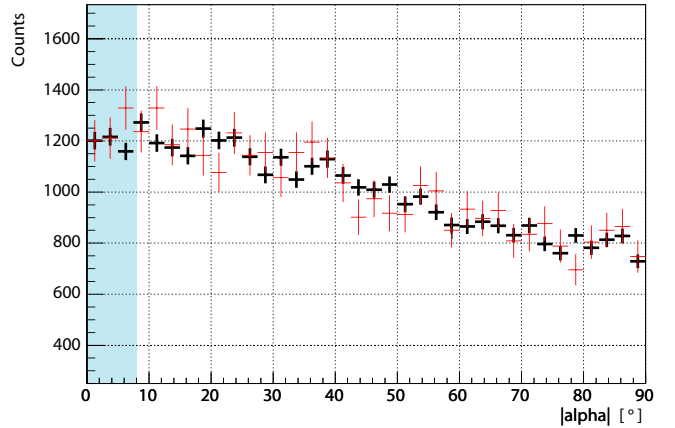


FIG. 1.— Distribution of the parameter  $|\text{ALPHA}|$  for events  $\gtrsim 280$  GeV. The distribution of OFF-source events (red) was normalized to the ON-source events (black) in between  $20^\circ$  and  $85^\circ$ . An excess due to  $\gamma$ -rays from PSR B1951+32 is expected for  $|\text{ALPHA}| < 7.5^\circ$  (shaded region).

taken into account. The upper limits on excess events were converted into upper limits on the integral flux by assuming a spectral index of 2.6 for the calculation of the effective collection areas. Note that the dependence of the effective collection area on the assumed spectral index can be generally neglected. The limits on the integral flux of  $\gamma$ -rays are shown in Figure 2 together with the measurement of Srinivasan et al. (1997) and the predictions of Bednarek and Bartosik (2003).

#### 3.2. Search for $\gamma$ -ray Emission in the Vicinity of PSR B1951+32

We explored the region in the sky around the position of the pulsar for a possible extended and/or displaced emission region of  $\gamma$ -rays. The latter is a likely scenario due to the high proper motion of the pulsar. For this study we employed the DISP-method by Fomin et al. (1994) with a modified parametrization (Domingo-Santamaria et al. 2005), which permits the reconstruction of the arrival direction of a  $\gamma$ -ray  $\gtrsim 100$  GeV with an accuracy of  $\sim 0.1^\circ$ . Sky maps were produced in different bins of energy. In none of the maps  $\gamma$ -ray emission was found within the reconstructed field of view of  $\sim 0.6^\circ$  radius.

The map in Figure 3 shows the significance calculated in bins of  $(0.1 \times 0.1)$  degrees<sup>2</sup> for events with energies  $\gtrsim 200$  GeV. Figure 4 shows a map of the calculated upper limits (95 % Confidence Level) on the integral flux for the same events. The acceptance of the MAGIC camera was modelled using the radial dependence of the background rate in the camera after event selection. By comparing with MC simulations we confirmed for various angular distances from the camera center that the radial dependence of the background rate is compatible with the simulated  $\gamma$ -ray acceptance.

Following our study we can exclude steady  $\gamma$ -ray emission  $> 200$  GeV on the level predicted by Bednarek and Bartosik (2003), which we would have detected if a) the emission had been originating from within a circle of radius  $\approx 0.4^\circ$  centered on the position of the pulsar, and b) the apparent emission region had been restricted to less than  $\sim 0.3^\circ$  in diameter.

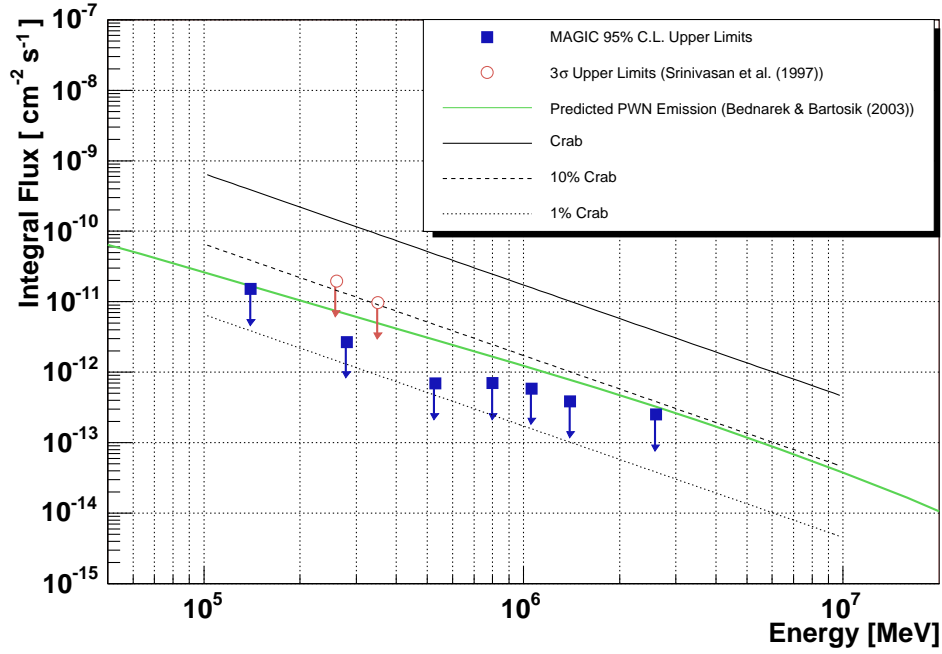


FIG. 2.— Integral upper limits (95 % Confidence Level) on the steady  $\gamma$ -ray emission from the direction of PSR B1951+32. For comparison, the  $\gamma$ -ray flux of the Crab nebula (Wagner et al. 2005) is also indicated.

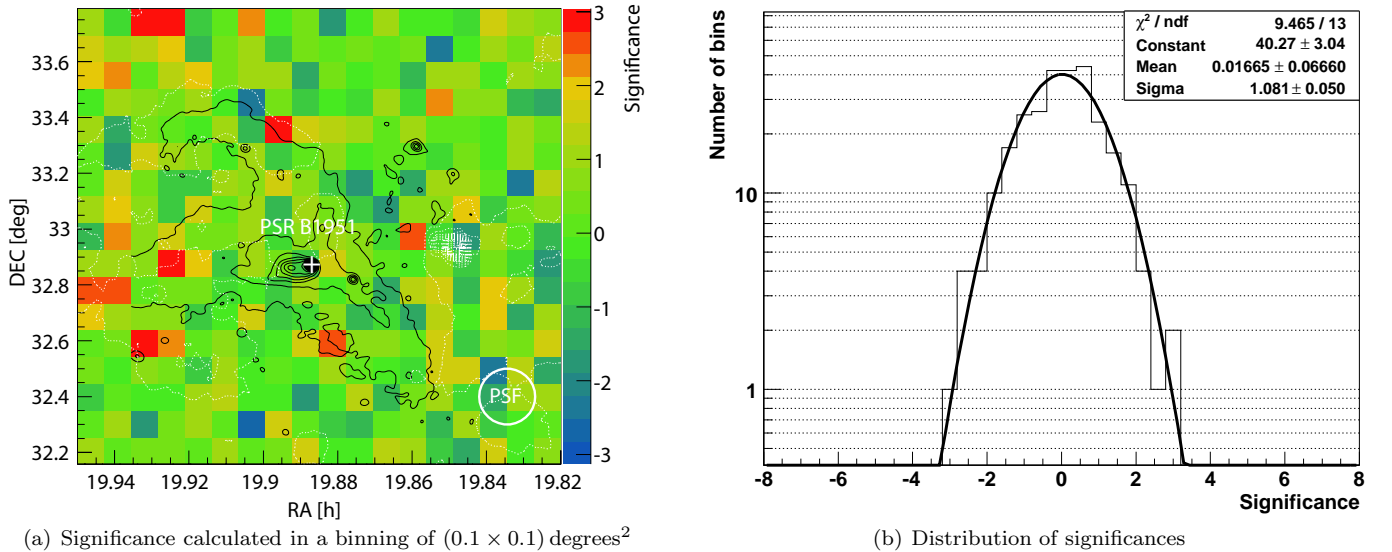


FIG. 3.— Significance of VHE  $\gamma$ -ray emission from the region around PSR B1951+32. Left Side: calculated significance of VHE  $\gamma$ -ray emission  $\gtrsim 200$  GeV in bins of  $(0.1 \times 0.1)$  degrees<sup>2</sup>. Overlaid in black are contours of observations at radio (Castelleti et al. 2003) and in white contours of IR observations (Fesen et al. 1988). Right Side: distribution of significances. The distribution has a mean of 0.01 and a RMS of 1.08, compatible with randomly distributed data.

### 3.3. Search for pulsed Emission

The time of each event (hereafter arrival time) is derived from the time signal of a GPS-controlled Rubidium clock with a precision of  $\sim 200$  nanoseconds. Before we searched for pulsed emission from the pulsar, the arrival times were transformed to the barycenter of the solar system with the TEMPO timing package (Taylor et al. 2000). Afterwards, the corrected arrival times  $t_j$  were

folded to the corresponding phase  $\phi_j$  of PSR B1951+32:

$$\phi_j = \nu(t_j - t_0) + \frac{1}{2}\dot{\nu}(t_j - t_0)^2 + \frac{1}{6}\ddot{\nu}(t_j - t_0)^3$$

where  $\nu$ ,  $\dot{\nu}$ ,  $\ddot{\nu}$  and  $t_0$  are the values of a contemporary ephemeris provided by Lyne (2006), which is listed in Table 3. The analysis chain that was set up to search for pulsed emission was previously tested on data from optical observation of the Crab pulsar with the central pixel (CP) of the MAGIC camera (Lucrelli et al. 2005). Details about the optical observation can be found in



TABLE 2  
RESULTS OF THE ANALYSIS IN SEARCH FOR STEADY  $\gamma$ -RAY EMISSION FROM PSR B1951+32.

Analysis Threshold [GeV]	ON Events	OFF Events	Excess Events	Significance [ $\sigma$ ]	Upper Limit Excess Events 95% C.L.	Flux Upper Limit [ $\text{cm}^{-2}\text{s}^{-1}$ ]
> 140	37869	$37933 \pm 381$	-64	-0.2	792	$1.5 \times 10^{-11}$
> 280	3576	$3740 \pm 150$	-164	-1.0	196	$2.7 \times 10^{-12}$
> 530	712	$777 \pm 42$	-65	-1.3	54	$7.0 \times 10^{-13}$
> 800	232	$231.5 \pm 22$	0.5	0.0	55	$7.0 \times 10^{-13}$
> 1060	101	$90.6 \pm 14$	10.4	0.6	45	$5.8 \times 10^{-13}$
> 1400	58	$49.5 \pm 10.8$	8.5	0.6	35	$3.9 \times 10^{-13}$
> 2600	17	$26 \pm 10$	-9	-0.9	14	$2.5 \times 10^{-13}$

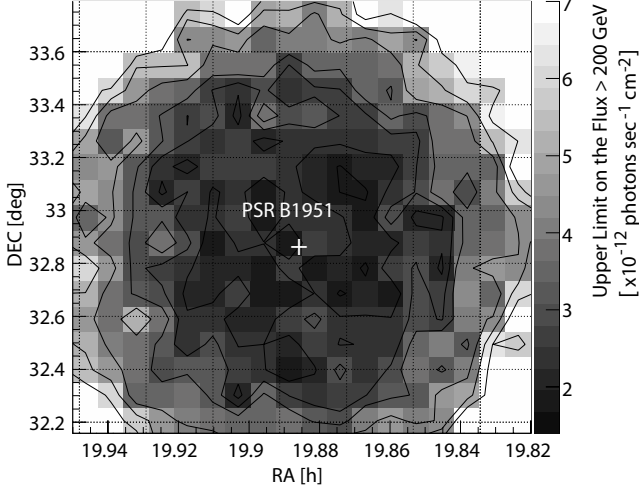


FIG. 4.— Upper limits (95 % Confidence Level) on the integral  $\gamma$ -ray emission  $> 200$  GeV, calculated in bins of  $(0.1 \times 0.1)$  degrees<sup>2</sup>.

Lucarelli et al. (2007).

TABLE 3  
EPHEMERIS OF PSR B1951+32 FROM LYNE (2006).  
UNCERTAINTIES ARE GIVEN IN BRACKETS.

<b>Position Epoch</b>	2450228.4144 JD
<b>Right Ascension</b>	$19^{\text{h}}52^{\text{m}}58^{\text{s}}.27568995$
<b>Declination</b>	$32^{\circ}52'40''6824033$
<b>Pulsar Epoch</b>	2453931.724208 JD
$\nu$	$25.29516019929(63)$ Hz
$\dot{\nu}$	$-3.72818(33) \cdot 10^{-12}$ Hz/s
$\ddot{\nu}$	$-1.15(25) \cdot 10^{-21}$ Hz/s <sup>2</sup>

We performed a search for pulsed  $\gamma$ -ray emission from PSR B1951+32 in 5 differential bins of reconstructed energy between 100 GeV and 2 TeV. To test for periodicity we applied the Pearson- $\chi^2$ -test, the H-Test (de Jager et al. 1989) and the test by Gregory and Lored (1992) (hereafter Bayesian-Test). No signature of pulsed emission was found in any of the energy intervals. As an example we give the results of the H-Test, which yielded significances of 0.3, 2.3, 0.6, 0.2 and  $1.4\sigma$  respectively with increasing energy. The corresponding 95% confidence level upper limits on pulsed emission are shown in Figure 5. The limits were calculated from the results of the H-Test (de Jager 1994) by assuming a duty cycle of the pulsed emission of 36%, which corresponds to the duty cycle of PSR B1951+32 at energies  $> 100$  MeV (Ramanamurthy et al. 1995). A spectral slope of 2.6 was assumed in the calculation of the collection area. Note that these are upper limits in

differential bins of energy whereas the upper limits from Whipple (Srinivasan et al. 1997) are integral ones, which were converted to differential ones assuming a spectral shape of 2.6.

In a second analysis, we searched for pulsed emission by selecting events with a SIZE  $> 100$  photoelectrons<sup>24</sup>, i.e. events with energies  $\gtrsim 75$  GeV. Again, no hint of pulsed emission was found. The H-Test yielded 1.4, and a  $\chi^2$ -Test 7.2 with 11 degrees of freedom. The test by Gregory and Lored (1992) gave a probability for pulsed emission of  $2.4 \cdot 10^{-4}$ .

From the result of the H-Test we calculated an upper limit on the number of excess events (s. Table 4), from which we derived an upper limit on the cutoff energy of the pulsed emission in the following way. The known spectrum of PSR B1951+32 at GeV energies, measured by EGRET (Fierro 1996), was multiplied with an exponential cutoff and convoluted with the effective collection area of the telescope. For a given cutoff energy we then obtained the number of expected excess events by multiplying the result with the dead-time corrected observation time. The upper limit on the cutoff energy was finally found by iteratively changing the cutoff energy until the number of expected excess events matched the upper limit on the number of pulsed excess events. With this procedure we obtained an upper limit on the cutoff energy of 32 GeV. The effective collection area was calculated by assuming the EGRET measured spectral shape extrapolated with the same cutoff energy by which the collection area was convoluted. The measured spectrum of PSR B1951+32 multiplied by an exponential cutoff of 32 GeV is shown as a solid red line in Figure 5. The analysis threshold, 75 GeV, is marked with the red arrow in the figure.

As a crosscheck the same analysis was repeated, this time by selecting all events with a SIZE  $< 300$  photoelectrons, i.e. events with energies  $\lesssim 180$  GeV. The resulting phasogram in Figure 6 shows no evidence for pulsed emission. From this analysis resulted a slightly better upper limit on the cutoff energy of 28 GeV. The analysis threshold, 60 GeV, was lower because also events with a SIZE below 100 photoelectrons have been included in the analysis.

#### 4. DISCUSSION

Theoretical predictions and experimental evidence from lower energies had been quite favorable for a possi-

<sup>24</sup> SIZE is the integrated intensity of a shower image after applied tail-cuts in units of photoelectrons. It is also a good reason of the incident energy from shower impact parameters between  $\sim 50$  to 120 m

TABLE 4  
RESULTS OF THE ANALYSIS FOR PERIODICITY.

	Result	Significance	H-Test	$2\sigma$ Flux U.L. [ $\text{cm}^{-2}\text{s}^{-1}$ ]	$\chi^2$	Bayesian test
			$2\sigma$ U.L. Excess Events			
SIZE > 100 phe	1.4	$0.3\sigma$	2188	$4.3 \cdot 10^{-11}$	7.2	$2.4 \cdot 10^{-4}$
SIZE < 300 phe	3.2	$1.1\sigma$	3388	$5.0 \cdot 10^{-11}$	10.7	$3.6 \cdot 10^{-4}$

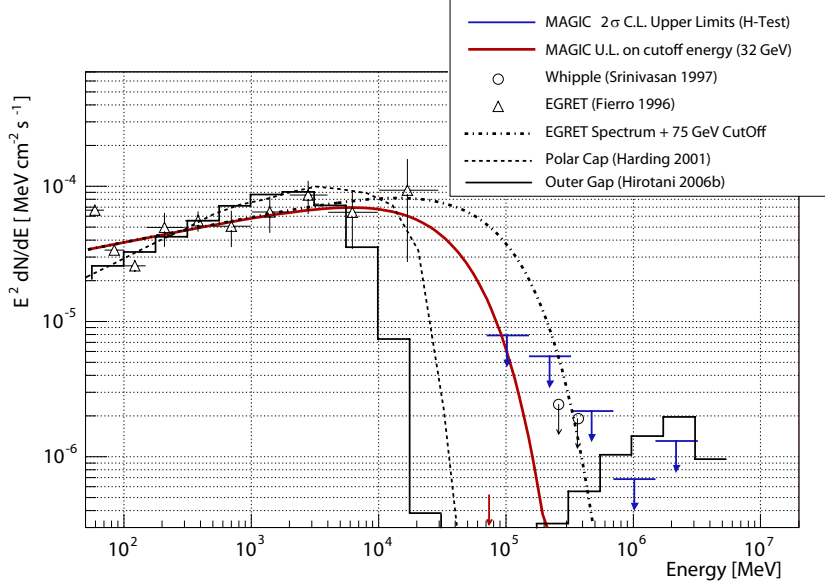


FIG. 5.— Results of the analysis in the search for pulsed emission from PSR B1951+32. Upper limits are given with a 95 % confidence level. The upper limit on the cutoff energy from Whipple is shown as the dot dashed curve. The upper limit on the cutoff of 32 GeV by MAGIC is shown as the solid red curve. The analysis threshold (75 GeV) is marked by the arrow on the X-Axis.

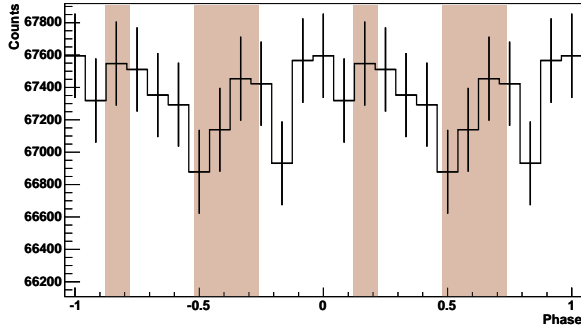


FIG. 6.— Phasogram of PSR B1951+32 obtained after selecting events with a SIZE < 300 photoelectrons. The shaded areas indicate the phase regions in which PSR B1951+32 is emitting at GeV energies (Ramanamurthy et al. 1995).

ble detection of  $\gamma$ -ray emission from PSR B1951+32 or its nebula with MAGIC. Nevertheless, despite the higher sensitivity of this observation compared to previous ones, no  $\gamma$ -ray emission was detected.

The upper limits in Figure 2 on the steady  $\gamma$ -ray emission from the PWN surrounding PSR 1951+32 are below the  $\gamma$ -ray flux that was predicted by the time dependent model of Bednarek and Bartosik (2003, 2005a). Although their model takes into account the temporal evolution of the nebula (but not the spatial evolution), the acceleration of leptons and therefore also the equilibrium spectrum of leptons inside the nebula still depends on a few free parameters, which are usually not well known. These parameters, e.g. the density of the medium surrounding the PWN, the acceleration efficiency of lep-

tons, or the magnetization parameter of the pulsar wind at the shock region, need reasonable guesses in order to estimate the  $\gamma$ -ray flux.

Concerning the magnetization parameter, i.e. the ratio of the magnetic energy flux to the particle energy flux, Li et al. (2005) have recently estimated the magnetic field strength of the compact X-ray nebula around PSR B1951+32 to be  $\sim 300 \mu\text{G}$ , which is larger than the value assumed by Bednarek and Bartosik. At the present time it is therefore clear that the value of the magnetization parameter  $\sigma$  of the pulsar wind has to be much larger than the value of  $\sigma = 10^{-3}$ , which Bednarek and Bartosik assumed. As a result, the cooling of electrons by synchrotron radiation is faster and the IC  $\gamma$ -ray flux is suppressed. Nevertheless, a hadronic component, as predicted in some models (Bednarek and Bartosik 2003; Horns et al. 2006) which would dominate if the acceleration efficiency of leptons was low (Bednarek 2006), would be below the sensitivity of our observation.

Another aspect is that the model of Bednarek and Bartosik deals with PWNe which are well confined by the external medium, and pulsars which are, at most, moving slowly through the interstellar medium (the prototype of such a nebula is the Crab nebula). Only in such a scenario a well localized  $\gamma$ -ray source should be expected, whereas, when the pulsar is moving very fast, the  $\gamma$ -ray emission will be distributed over a larger volume. In the case of PSR B1951+32, which is moving with an apparent velocity of  $240 \pm 40 \text{ km s}^{-1}$  (Migliazzo et al. 2002), the  $\gamma$ -ray flux

estimated by Bednarek and Bartosik (2005b) will be smeared over an area with a diameter of at least  $\sim 0.5$  degrees (assuming an age of the pulsar of  $7 \times 10^4$  years), which reduces the detection probability with MAGIC. In this context it is interesting to note that extended TeV  $\gamma$ -ray sources associated with displaced pulsars, were recently detected by the H.E.S.S. Collaboration (e.g. the Vela pulsar Aharonian et al. (2006) or PSR B1823-13 Aharonian et al. (2005)).

Considering the  $\gamma$ -ray emission from the pulsar, we constrain the cutoff of the pulsed emission to  $< 32$  GeV for the case that the cutoff is an exponential. Regarding further that large uncertainties govern the last spectral point measured by EGRET it follows that the allowed energy region where the cutoff resides can be constrained to lie somewhere between 10 and 30 GeV. The narrow allowed range does not leave much freedom for models. This result and the upper limits from the search in differential bins of energy are compared in Figure 5 with theoretical predictions from the polar-cap and the outer-gap model. In the figure, the dotted line represents the polar-cap predictions from (Harding 2001), renormalized to the points of the EGRET spectrum. The thin solid line shows the spectrum of a latest outer-gap model (Hirotani 2006b).

The polar-cap model predicts a cutoff in the curvature radiation which is within the allowed region whereas the outer-gap model seems to marginally underestimate the cutoff energy. Nevertheless it has to be emphasized that in both models the spectral cutoff sensitively depends on model parameters and assumptions which have to be made because of insufficient experimental constraints as well as incomplete theories about the pulsar magnetosphere. Therefore, in order to resolve the longstanding question about the cutoff in the curvature spectra, upcoming measurements are needed with higher statis-

tics around 10 GeV e.g. by GLAST or measurements by future ground based experiments with lower thresholds than MAGIC e.g. MAGIC II or CTA.

Furthermore the predicted inverse-Compton (IC) flux at TeV-energies in the outer-gap model appears to be inconsistent with our upper limits. Nevertheless it must be noted that the IC-flux is obtained by assuming that all the magnetospheric soft photons illuminate the equatorial region of the magnetosphere in which the gap-accelerated positrons are migrating outwards. Therefore the predicted IC-flux as a function of energy specifies an upper boundary of the possible pulsed TeV emission. However, the poloidal magnetic field lines could be more or less straight near the light cylinder, as the solution of the time-dependent force-free electrodynamics of an oblique rotator indicates (Spitkovsky 2006). If this is the case, soft photons from the magnetosphere will not be efficiently upscattered and the IC flux will be significantly reduced. This problem will be solved in future when the self-consistent gap electrodynamics (Hirotani 2006a,b) and the three-dimensional force-free electrodynamics will be combined.

## 5. ACKNOWLEDGMENTS

We are grateful for the preparation of the ephemeris of PSR B1951+32 by Andrew Lyne, thus enabling us to perform the pulsed analysis. Alice Harding was so kind as to provide us with her polar cap predictions of PSR B1951+32. We also would like to thank the IAC for the excellent working conditions at the ORM in La Palma. The support of the German BMBF and MPG, the Italian INFN, the Spanish CICYT, ETH research grant TH 34/04 3, and the Polish MNiI grant IP03D01028 are gratefully acknowledged.

## REFERENCES

- F. Aharonian, et al. *A&A*, 448:L43–L47, March 2006. doi: 10.1051/0004-6361:200600014.
- F. A. Aharonian, et al. *A&A*, 442:L25–L29, November 2005. doi: 10.1051/0004-6361:200500180.
- A. M. Atoyan and F. A. Aharonian. *MNRAS*, 278:525–541, January 1996.
- W. Bednarek. *ArXiv Astrophysics e-prints*, October 2006.
- W. Bednarek and M. Bartosik. *A&A*, 405:689–702, July 2003. doi: 10.1051/0004-6361:20030593.
- W. Bednarek and M. Bartosik. In F. A. Aharonian, H. J. Völk, and D. Horns, editors, *AIP Conf. Proc. 745: High Energy Gamma-Ray Astronomy*, pages 329–334, February 2005a.
- W. Bednarek and M. Bartosik. *Journal of Physics G Nuclear Physics*, 31:1465–1474, December 2005b. doi: 10.1088/0954-3899/31/12/008.
- R. K. Bock, et al. *Nuclear Instruments and Methods in Physics Research A*, 516:511–528, January 2004. doi: 10.1016/S0168-9002(03)02505-1.
- L. Breiman. *Machine Learning*, 45:5–32, 2001. doi: 10.1023/A:1010933404324.
- G. Castelletti, G. Dubner, K. Golap, W. M. Goss, P. F. Velazquez, M. Holdaway, and A. P. Rao. *ArXiv Astrophysics e-prints*, October 2003.
- K. S. Cheng, C. Ho, and M. Ruderman. *ApJ*, 300:500–539, January 1986a. doi: 10.1086/163829.
- K. S. Cheng, C. Ho, and M. Ruderman. *ApJ*, 300:522–+, January 1986b. doi: 10.1086/163830.
- J. Chiang and R. W. Romani. *ApJ*, 400:629–637, December 1992. doi: 10.1086/172024.
- J. Cortina et al. In *International Cosmic Ray Conference*, pages 359–+, 2005.
- J. K. Daugherty and A. K. Harding. *ApJ*, 252:337–347, January 1982. doi: 10.1086/159561.
- O. C. de Jager. *ApJ*, 436:239–248, November 1994. doi: 10.1086/174896.
- O. C. de Jager and A. K. Harding. *ApJ*, 396:161–172, September 1992. doi: 10.1086/171706.
- O. C. de Jager, B. C. Raubenheimer, and J. W. H. Swanepoel. *A&A*, 221:180–190, August 1989.
- E. Domingo-Santamaria et al. In *International Cosmic Ray Conference*, pages 363–+, 2005.
- R. A. Fesen, J. M. Saken, and J. M. Shull. *Nature*, 334:229–231, July 1988. doi: 10.1038/334229a0.
- J. M. Fierro. *Ph.D. Thesis*, 1996.
- V. P. Fomin, A. A. Stepanian, R. C. Lamb, D. A. Lewis, M. Punch, and T. C. Weekes. *Astroparticle Physics*, 2:137–150, May 1994. doi: 10.1016/0927-6505(94)90036-1.
- M. Gaug et al. In *International Cosmic Ray Conference*, pages 375–+, 2005.
- P. C. Gregory and T. J. Lored. *ApJ*, 398:146–168, October 1992. doi: 10.1086/171844.
- A. K. Harding. In F. A. Aharonian and H. J. Völk, editors, *American Institute of Physics Conference Series*, pages 115–+, 2001.
- A. K. Harding, M. G. Baring, and P. L. Gonthier. *ApJ*, 476:246–+, February 1997. doi: 10.1086/303605.
- A. K. Harding, E. Tadamaru, and L. W. Esposito. *ApJ*, 225:226–236, October 1978. doi: 10.1086/156486.
- A. M. Hillas. In F. C. Jones, editor, *International Cosmic Ray Conference*, pages 445–448, August 1985.
- K. Hirotani. in press. *ApJ*, 2006a.
- K. Hirotani. paper in preparation. 2006b.

- D. Horns, F. Aharonian, A. Santangelo, A. I. D. Hoffmann, and C. Masterson. *A&A*, 451:L51–L54, June 2006. doi: 10.1051/0004-6361:200651116.
- S. R. Kulkarni, T. C. Clifton, D. C. Backer, R. S. Foster, and A. S. Fruchter. *Nature*, 331:50–53, January 1988. doi: 10.1038/331050a0.
- X. H. Li, F. J. Lu, and T. P. Li. *ApJ*, 628:931–937, August 2005. doi: 10.1086/430941.
- E. Lorenz. *New Astronomy Review*, 48:339–344, April 2004. doi: 10.1016/j.newar.2003.12.059.
- F. Lucarelli et al. In *International Cosmic Ray Conference*, pages 367–+, 2005.
- F. Lucarelli et al. 2007. In preparation.
- A. Lyne. Private Communication, 2006.
- R. N. Manchester, G. B. Hobbs, A. Teoh, and M. Hobbs. The Australia Telescope National Facility Pulsar Catalogue. *AJ*, 129:1993–2006, April 2005. doi: 10.1086/428488. URL <http://www.atnf.csiro.au/research/pulsar/psrcat/>.
- J. M. Migliazzo, B. M. Gaensler, D. C. Backer, B. W. Stappers, E. van der Swaluw, and R. G. Strom. *ApJ*, 567:L141–L144, March 2002. doi: 10.1086/340002.
- D.-S. Moon, et al. *ApJ*, 610:L33–L36, July 2004. doi: 10.1086/423238.
- P. V. Ramanamurthy, et al. *ApJ*, 447:L109+, July 1995. doi: 10.1086/309572.
- W. A. Rolke, A. M. López, and J. Conrad. *Nuclear Instruments and Methods in Physics Research A*, 551:493–503, October 2005. doi: 10.1016/j.nima.2005.05.068.
- A. Spitkovsky. *ApJ*, 648:L51–L54, September 2006. doi: 10.1086/507518.
- R. Srinivasan, et al. *ApJ*, 489:170–+, November 1997. doi: 10.1086/304781.
- J. H. Taylor, R. N. Manchester, D. J. Nice, J. M. Weisberg, Irwin A., and Wex N. Tempo pulsar timing package, 2000. URL <http://www.atnf.csiro.au/research/pulsar/tempo/>.
- R. M. Wagner et al. In *International Cosmic Ray Conference*, pages 163–+, 2005.